

Antagonism of the chemokine Ccl5 ameliorates experimental liver fibrosis in mice

Marie-Luise Berres,¹ Rory R. Koenen,² Anna Rueland,¹ Mirko Moreno Zaldivar,¹ Daniel Heinrichs,¹ Hacer Sahin,¹ Petra Schmitz,¹ Konrad L. Streetz,¹ Thomas Berg,³ Nikolaus Gassler,⁴ Ralf Weiskirchen,⁵ Amanda Proudfoot,⁶ Christian Weber,² Christian Trautwein,¹ and Hermann E. Wasmuth¹

¹Medical Department III and ²Institute of Molecular Cardiovascular Research, University Hospital Aachen, Aachen, Germany. ³Department of Gastroenterology and Hepatology, Charité University Hospital Berlin, Berlin, Germany. ⁴Institute of Pathology and ⁵Institute of Clinical Chemistry and Pathobiochemistry, University Hospital Aachen, Aachen, Germany. ⁶Merck Serono Geneva Research Centre, Geneva, Switzerland.

Activation of hepatic stellate cells in response to chronic inflammation represents a crucial step in the development of liver fibrosis. However, the molecules involved in the interaction between immune cells and stellate cells remain obscure. Herein, we identify the chemokine CCL5 (also known as RANTES), which is induced in murine and human liver after injury, as a central mediator of this interaction. First, we showed in patients with liver fibrosis that CCL5 haplotypes and intrahepatic CCL5 mRNA expression were associated with severe liver fibrosis. Consistent with this, we detected Ccl5 mRNA and CCL5 protein in 2 mouse models of liver fibrosis, induced by either injection of carbon tetrachloride (CCl₄) or feeding on a methionine and choline-deficient (MCD) diet. In these models, Ccl5^{-/-} mice exhibited decreased hepatic fibrosis, with reduced stellate cell activation and immune cell infiltration. Transplantation of Ccl5-deficient bone marrow into WT recipients attenuated liver fibrosis, identifying infiltrating hematopoietic cells as the main source of Ccl5. We then showed that treatment with the CCL5 receptor antagonist Met-CCL5 inhibited cultured stellate cell migration, proliferation, and chemokine and collagen secretion. Importantly, in vivo administration of Met-CCL5 greatly ameliorated liver fibrosis in mice and was able to accelerate fibrosis regression. Our results define a successful therapeutic approach to reduce experimental liver fibrosis by antagonizing Ccl5 receptors.

Introduction

Chronic liver diseases are a major cause of mortality and morbidity worldwide. Among chronic liver injuries, chronic hepatitis C virus infection and nonalcoholic steatohepatitis (NASH) are the most common entities in the United States and Europe leading to liver fibrosis and end-stage liver disease, including hepatocellular carcinoma (1). In these diseases, liver fibrosis is considered as the result of a chronic wound healing response to a continuous hepatocellular insult, which results in an inflammatory response within the liver and the subsequent activation of hepatic stellate cells, which produce an excess of extracellular matrix proteins (2, 3). Established liver fibrosis has long been considered as a static process, but this concept has recently been challenged by the finding that fibrosis and even cirrhosis are reversible in a considerable number of cases (4). These results have fuelled the enthusiasm that key pathways might be defined, whose modulation bears the potential to influence the natural history of chronic liver diseases and to induce fibrosis regression.

The inflammatory response during chronic liver injury is a dynamic process with intrahepatic accumulation of diverse immune cells (T cells, macrophages, and dendritic cells) (5). The migration and positioning of these cells is determined by the pattern of chemokines and cytokines that are produced by hepatocytes, biliary epithelial cells, and endothelial cells (6, 7). Important new data also implicate hepatic stellate cells in the recruitment of immune cells to the sites of tissue injury (8). Notably, activated

stellate cells secrete large amounts of chemokines (CCL2, CCL3, CCL5, CCL11, CXCL8, CXCL9, and CXCL10), thereby shaping the magnitude and the quality of the immune response during fibrotic liver diseases (8). Out of these chemokines, CCL2 and, more recently, CXCL9 have been identified as important mediators of tissue scarring by their dual effects on hepatic stellate cells and the intrahepatic immune environment (9–11). However, no direct agonistic or antagonistic strategies have yet been developed to explore their specific contributions to tissue injury.

In the current study, we focus on CCL5 (also known as RANTES), a 7.8-kDa CC chemokine, which is strongly expressed in the human and murine liver upon injury (12, 13). CCL5 was initially considered a T cell-specific protein but has since been found to be produced by numerous cell types, including platelets, macrophages, endothelial, and stellate cells (14). CCL5 recruits T cells, dendritic cells, eosinophils, NK cells, mast cells, and basophils to sites of inflammation by interacting with 3 specific G protein-coupled receptors: CCR1, CCR3, and CCR5. Notably, CCR5 has already been described on isolated hepatic stellate cells, suggesting that these cells are a source as well as a target of CCL5 within the liver (13, 15). Moreover, 2 receptors binding CCL5, CCR1, and CCR5 have recently been identified to promote hepatic fibrosis in mice in vivo (13). CCL5 and its receptors have also been shown to have detrimental effects during other inflammatory diseases, including acute Con A-induced liver failure (16, 17) as well as atherosclerosis and obesity, which share common pathophysiological pathways with liver diseases (18, 19). These intriguing actions of CCL5 and the availability of the specific CCL5 receptor antagonist Met-CCL5 (20–22) render this chemokine particularly interesting for further investigations in human and experimental liver diseases.

Authorship note: Marie-Luise Berres and Rory R. Koenen contributed equally to this work.

Conflict of interest: The authors have declared that no conflict of interest exists.

Citation for this article: *J Clin Invest.* 2010;120(11):4129–4140. doi:10.1172/JCI41732.

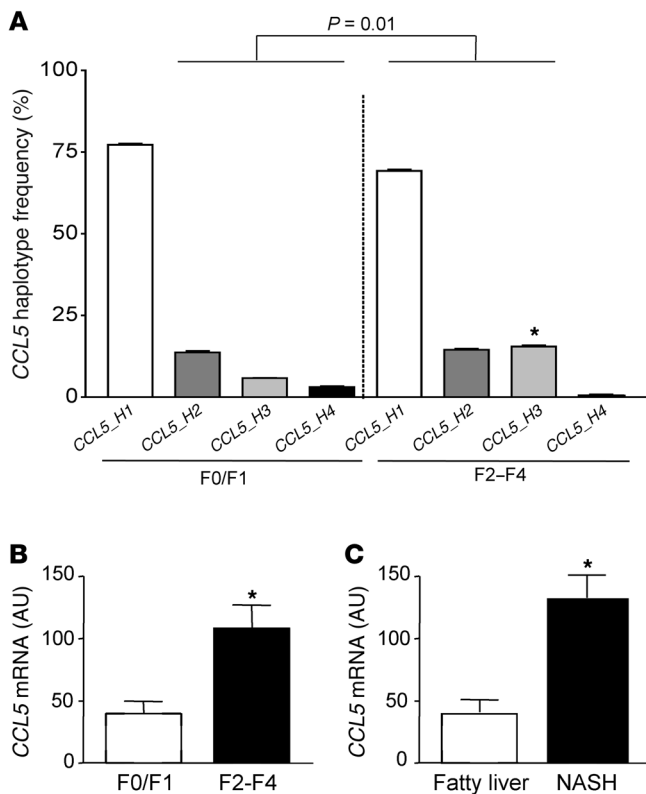


Figure 1

Association of *CCL5* with liver fibrosis in humans. **(A)** Haplotype analysis of the *CCL5* gene in patients with mild (stage F0/F1, $2n = 200$) or advanced (stage F2–F4, $2n = 222$) liver fibrosis. The overall haplotype distribution is significantly different between patients with mild fibrosis versus subjects with severe fibrosis ($P = 0.01$). Specifically, the third most common haplotype, *CCL5_H3*, is significantly more prevalent in individuals with advanced fibrosis (15.4%) compared with patients with mild fibrosis (5.9%, OR 2.83; $*P < 0.05$). **(B)** *CCL5* mRNA expression is significantly elevated in subjects with advanced HCV-induced fibrosis compared with that of patients with only mild fibrosis ($*P < 0.05$). **(C)** The association of *CCL5* mRNA expression with liver fibrosis is confirmed in patients with fibrosis due to NASH ($*P < 0.05$).

Along with these previous findings, we here show that *CCL5* is crucially involved in liver fibrosis across species and that genetic deletion or pharmacological antagonism of its receptors using Met-*CCL5* ameliorates experimental liver fibrosis in vivo.

Results

The chemokine CCL5 is associated with progressive liver fibrosis in humans. We first evaluated a genetic association of *CCL5* with liver fibrosis in a cohort of HCV-infected patients recruited at a tertiary referral center (23). In this cohort, the distribution of current HapMap *CCL5* haplotypes was significantly different between subjects with mild fibrosis (F0/F1), compared with patients with advanced fibrosis (F2–F4; $P = 0.01$; Figure 1A), as determined by permutation testing, which corrects for multiple testing (24). The difference in overall haplotype distribution is due to a higher frequency of the third most prevalent haplotype (*CCL5_H3*) in patients with advanced fibrosis (15.4%) compared with that in subjects with minor fibrosis (5.9%, $P < 0.05$; Figure 1A). The presence of this haplotype is statistically associated with an odds ratio (OR) of 2.83 for having severe fibrosis. The disease-associated haplotype is tagged by rs11652536, which shows strong linkage disequilibrium with a functional *CCL5* promoter SNP (–28 G/C, rs2280788; <http://hapmap.ncbi.nlm.nih.gov/>). The latter SNP has already been shown to increase *CCL5* expression in a reporter assay (25), although we could only detect a tendency to slightly higher *CCL5* serum levels in subjects carrying the minor allele of rs11652536 in our study (Supplemental Figure 1; supplemental material available online with this article; doi:10.1172/JCI141732DS1). Nevertheless, the observed association of rs11652536 with the severity of fibrosis was validated in an independent cohort of HCV-infected subjects (Supplemental Table 1). After having shown a genetic association of *CCL5* with

liver fibrosis, we next investigated the intrahepatic mRNA expression of *CCL5* in different fibrotic liver diseases. As depicted in Figure 1B, the *CCL5* mRNA is significantly increased in HCV-infected liver with advanced fibrosis compared with liver samples with only mild fibrosis ($P < 0.05$). We confirmed the increased *CCL5* mRNA expression in liver samples from patients with NASH and fibrosis compared with that of subjects with only fatty liver but no fibrosis (Figure 1C; $P < 0.05$), indicating that *CCL5* expression is associated with fibrotic liver diseases of different etiologies.

Ccl5 expression is increased in animal models of experimental liver fibrosis. We next evaluated the intrahepatic expression of *Ccl5* in C57BL/6 WT mice subjected to 2 models of experimental liver fibrosis: carbon tetrachloride (CCl_4) injections and a methionine and choline-deficient (MCD) diet. In both models, *Ccl5* mRNA levels were significantly increased compared with those of untreated control mice (Figure 2A; $P < 0.01$ for all comparisons with untreated mice), which is in line with recently published data of bile duct ligation (13). Importantly, the observed increase of *Ccl5* mRNA levels in the livers of treated animals was confirmed by *Ccl5* protein levels (Figure 2B; $P < 0.01$ and $P < 0.001$, comparing CCl_4 and MCD mice with untreated mice, respectively). To assess whether infiltrating immune cells or liver resident cells predominantly express *Ccl5* in liver fibrosis, we generated bone marrow chimeras in which we transplanted *Ccl5*-knockout (*Ccl5*^{–/–}) bone marrow into WT recipients (*Ccl5*^{–/–} → WT mice) and WT bone marrow into *Ccl5*^{–/–} recipients (WT → *Ccl5*^{–/–} mice). Compared with that of control mice (WT bone marrow into WT recipients [WT → WT mice]) and WT → *Ccl5*^{–/–} mice, *Ccl5*^{–/–} → WT chimeras displayed strongly reduced *Ccl5* protein levels in the CCl_4 -damaged livers (both $P < 0.01$; Figure 2C). In order to further visualize which immune cells express *Ccl5*, we performed immunofluorescence staining for

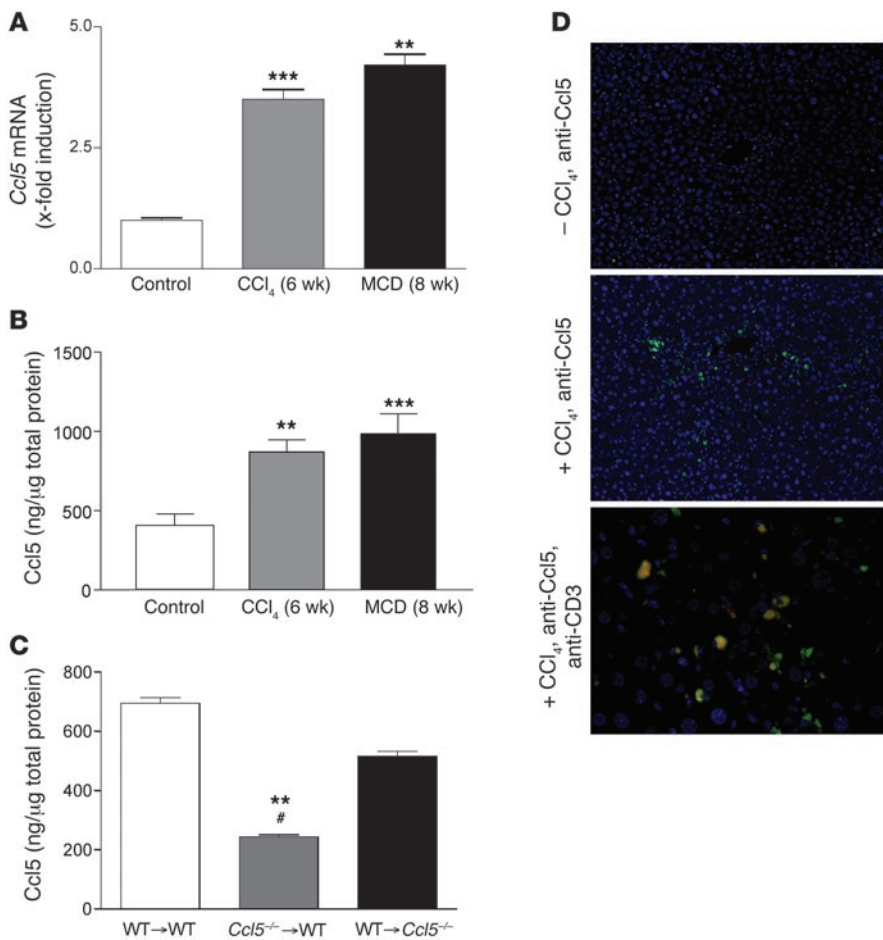


Figure 2

Association of Ccl5 with experimental liver fibrosis in mice. **(A)** *Ccl5* mRNA expression is significantly increased in total livers of mice treated with either CCl₄ for 6 weeks or the MCD diet for 8 weeks (***P* < 0.01, ****P* < 0.001). **(B)** The increased expression of *Ccl5* is also evident in the protein levels in both models of liver injury (***P* < 0.01, ****P* < 0.001). **(C)** Ccl5 protein content is significantly reduced in WT mice that received bone marrow from *Ccl5*^{-/-} mice (*Ccl5*^{-/-} → WT) after CCl₄ challenge compared with that of WT mice that received WT bone marrow (WT → WT) (***P* < 0.01) or *Ccl5*^{-/-} mice transplanted with WT bone marrow (WT → *Ccl5*^{-/-}) (#*P* < 0.05), suggesting that hematopoietic cells are the main source of Ccl5 during CCl₄-induced liver fibrosis. **(D)** Immunohistochemical detection of Ccl5 in the murine liver shows only faint staining in normal liver (original magnification, ×100 [top panel]). The expression of Ccl5 is predominantly increased around blood vessels after treatment with CCl₄ (original magnification, ×100 [middle panel]). Costaining with anti-CD3 (T cells) reveals that a significant number of Ccl5-positive cells are also positive for CD3 (original magnification, ×200 [bottom panel]).

Ccl5 in CCl₄-treated animals. Nontreated control livers showed only faint staining for Ccl5, but strong Ccl5 signals were detected around blood vessels after fibrosis induction (Figure 2D, top and middle panels). Costaining with anti-CD3 revealed that a significant number of Ccl5-positive cells are T cells infiltrating the damaged liver (Figure 2D, bottom panel).

Genetic deletion of Ccl5 reduces experimental liver fibrosis in vivo. In the light of these findings, we hypothesized that genetic deletion of *Ccl5* should lead to a reduced propensity of mice to develop liver fibrosis. We thus treated *Ccl5* WT and *Ccl5*^{-/-} animals with CCl₄ for 6 weeks to induce liver fibrosis. As shown in Figure 3A, *Ccl5*^{-/-} mice developed less severe liver fibrosis when compared with WT littermates. This difference was evident by a reduced Sirius red-positive area in histology (Figure 3A; *P* < 0.001) and reduced hepatic content of the collagen-specific amino acid hydroxyproline (Figure 3A; *P* < 0.05). ALT values were also significantly lower in the knockout animals (Figure 3B; *P* < 0.01) after 6 weeks CCl₄ treatment. The reduced ALT levels in *Ccl5*^{-/-} mice compared with those of WT mice were already evident 24 hours after a single injection of CCl₄ (Supplemental Figure 2A), suggesting an early reduction of inflammatory hepatocyte damage in *Ccl5*^{-/-} mice compared with their WT littermates.

To further establish the role of Ccl5 in experimental liver fibrosis, we determined the expression of pivotal fibrosis-related genes in the livers of *Ccl5*^{-/-} mice and their littermates after chronic CCl₄ administration. As depicted in Figure 3C, reduced liver fibrosis in mice lacking *Ccl5* was associated with altered expression of distinct

genes, which are strongly implicated in the deposition and turn over of extracellular matrix proteins. These include *Col1a1*, *Tgfb1*, *Mmp9*, *Timp1*, and the inflammatory cytokine *Il6* (26). As most of these genes have also been implicated in the biology of hepatic stellate cells (27), we also assessed the activation of these cells after treatment with CCl₄. In accordance with the former results, immunofluorescence staining of α-SMA revealed a strongly reduced number of α-SMA-positive cells within the livers of *Ccl5*^{-/-} mice compared with that of WT animals. This finding was confirmed by Western blot analysis of α-SMA in total liver extracts (Figure 3D), indicating that stellate cell activation is strongly reduced by genetic deletion of *Ccl5* in mice. This appears to be due to changes in immune-mediated activation, as the in vitro activation was not different between primary stellate cells isolated from WT versus *Ccl5*^{-/-} mice (Supplemental Figure 3). In line with these results, the inflammatory infiltrate was qualitatively changed in the *Ccl5*^{-/-} mice, which showed a significant reduction of intrahepatic macrophages and T cells after chronic CCl₄ administration (Supplemental Figure 2B).

Notably, we replicated our findings in the CCl₄ model of liver fibrosis in a dietary-induced liver damage model. After feeding the mice with a MCD diet for 8 weeks, *Ccl5*^{-/-} mice again showed reduced liver fibrosis compared with their WT littermates. This difference was evident upon histological examination and was confirmed by significantly reduced hydroxyproline levels (Figure 3E). As in the CCl₄ model, *Ccl5*^{-/-} mice also had reduced ALT values (Figure 3F; *P* < 0.01) and a repression of profibrotic mRNA expression (Figure 3G) compared

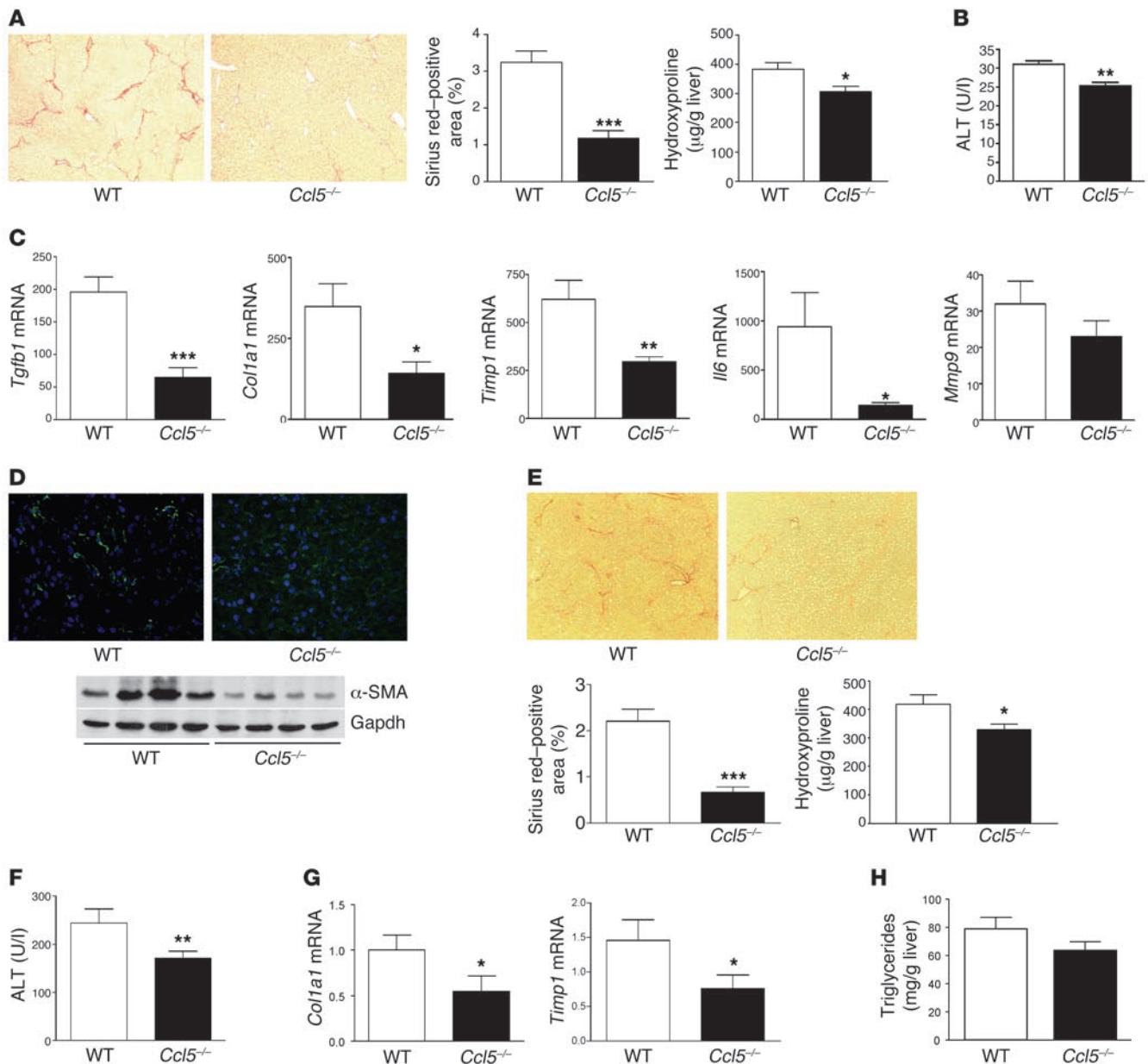
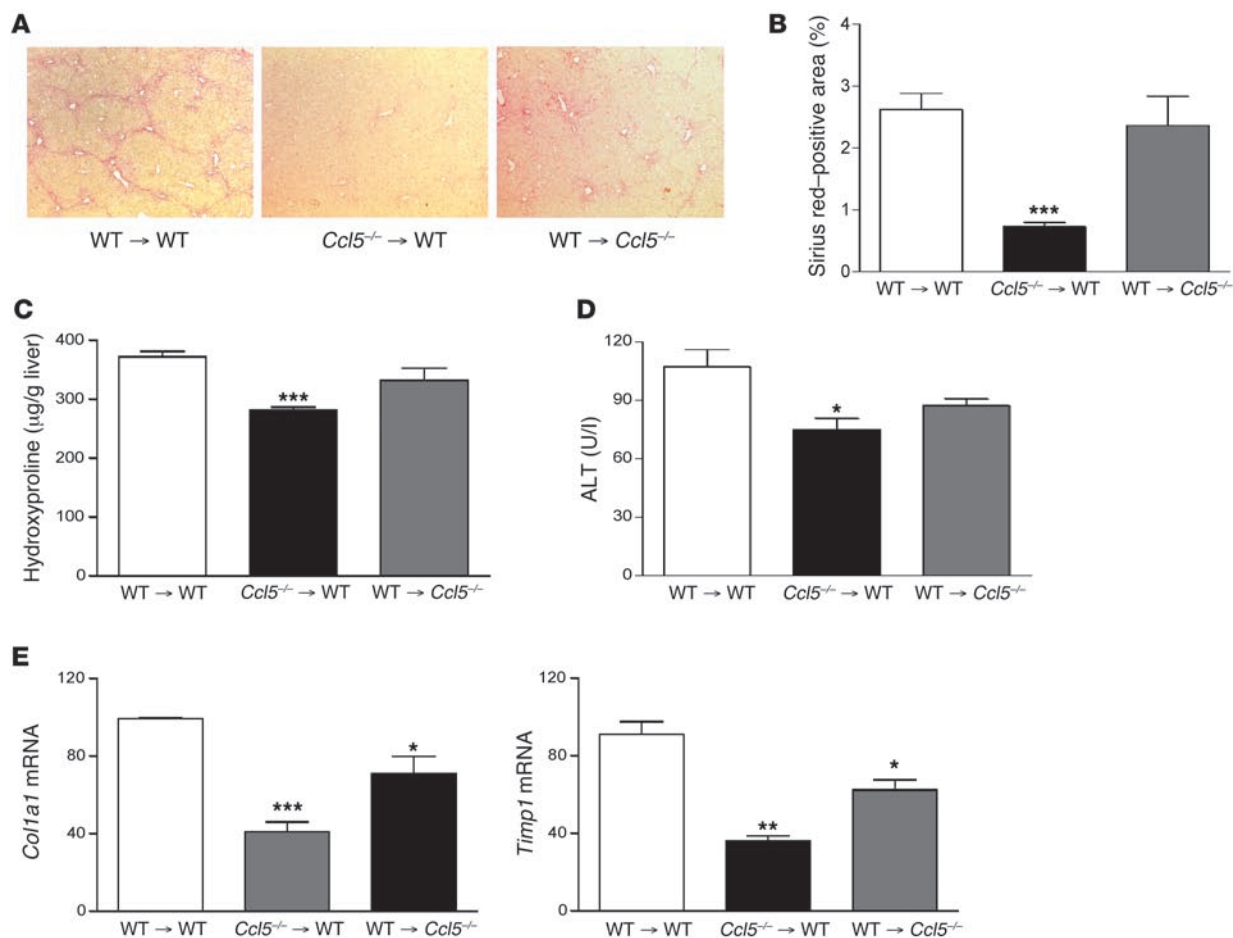


Figure 3

Experimental liver fibrosis in *Ccl5*-knockout mice. (A) Representative Sirius red stainings of WT and *Ccl5*^{-/-} mice after challenge with CCl₄ (original magnification, ×40). Reduced fibrosis in *Ccl5*^{-/-} mice (*n* = 12/group) is validated by the significantly lower Sirius red-positive area (****P* < 0.001) and decreased hydroxyproline concentrations (**P* < 0.05). (B) *Ccl5*^{-/-} mice also have lower ALT values compared with WT littermates (***P* < 0.01). (C) Treatment of *Ccl5*^{-/-} mice with CCl₄ leads to significantly reduced mRNA levels of *Col1a1*, *Tgfb1*, *Timp1*, and *Il6* (all with *P* values of at least < 0.05; **P* < 0.05, ***P* < 0.01, ****P* < 0.001), compared with WT mice. (D) Immunohistochemistry demonstrates reduced α-SMA-positive cells within the livers of *Ccl5*^{-/-} mice compared with WT mice after induction of liver fibrosis (original magnification, ×100). Decreased α-SMA protein expression is also evident in liver lysates of *Ccl5*^{-/-} mice (representative samples). (E) Ameliorated fibrogenesis in *Ccl5*^{-/-} mice (*n* = 12/group) is confirmed in the MCD diet model of liver fibrosis, as shown by representative Sirius red stainings (original magnification, ×40). Decreased deposition of collagen in *Ccl5*^{-/-} animals is validated by the reduced Sirius red-positive area (****P* < 0.001) and lower hydroxyproline concentrations (**P* < 0.05). (F) As in the CCl₄ model, ALT values are also reduced in *Ccl5*^{-/-} mice after feedings with the MCD diet (***P* < 0.01). (G) Likewise, *Col1a1* and *Timp1* mRNA is reduced in *Ccl5*^{-/-} mice compared with their littermates after feedings with MCD diet for 8 weeks (**P* < 0.05). (H) Furthermore, *Ccl5*^{-/-} mice show a trend toward lower hepatic triglyceride levels (*P* = 0.1).

with WT animals. *Ccl5*^{-/-} mice also had a tendency toward reduced hepatic triglyceride levels compared with their WT littermates (Figure 3H; *P* = 0.1), suggesting that *Ccl5* might also have effects on metabolic parameters in steatohepatitis-associated fibrosis.

Deletion of Ccl5 from hematopoietic cells is sufficient to ameliorate liver fibrosis in vivo. CCL5 is secreted by liver resident cells (8, 13) as well as infiltrating immune cells (14). In order to clarify which cells are targets and which are the main source of *Ccl5*, we performed bone

**Figure 4**

Bone marrow chimeric mice. (A) WT mice that receive bone marrow from *Ccl5*^{-/-} mice display significantly reduced liver fibrosis compared with *Ccl5*^{-/-} or WT animals transplanted with WT bone marrow ($n = 7-8/\text{group}$; original magnification, $\times 40$) (B) The reduced propensity to liver damage of *Ccl5*^{-/-} → WT mice is also shown by a lower Sirius red-positive area on histology ($***P < 0.001$), (C) reduced hydroxyproline liver contents ($***P < 0.001$), and (D) lower ALT values ($*P < 0.05$). (E) The mRNA expression of fibrosis-related genes, *Col1a1*, *Timp1*, and *Tgfb1*, is also strongly reduced in *Ccl5*^{-/-} → WT mice compared with that of the other groups ($***P < 0.001$, $**P < 0.01$, $*P < 0.05$).

marrow transplantation experiments in which *Ccl5*^{-/-} bone marrow was reconstituted into WT recipients (*Ccl5*^{-/-} → WT mice) and vice versa (WT → *Ccl5*^{-/-} mice) after lethal irradiation. WT mice transplanted with WT bone marrow (WT → WT mice) served as controls in these experiments. All transplanted mice were subjected to the CCL₄ fibrosis model for 6 weeks. As depicted in Figure 4, transplantation of WT bone marrow into *Ccl5*^{-/-} recipients (WT → *Ccl5*^{-/-} mice) only led to an moderate reduction of liver fibrosis compared with that of WT → WT mice. In contrast, WT mice that received bone marrow from *Ccl5*^{-/-} donors showed strongly reduced liver scarring as evidenced by histology, hydroxyproline levels, and a repression of pivotal profibrotic gene mRNA expression (Figure 4). These results further supported our hypothesis that Ccl5 expression by infiltrating immune cells is required for development of liver fibrosis after toxic injury.

Met-CCL5 antagonizes effects of CCL5 on stellate cells. As the bone marrow chimera experiments suggested that liver infiltrating cells are a potent source of Ccl5 (Figure 2C), we next assessed the direct biological effects of CCL5 and the CCL5 receptor antagonist Met-CCL5 on immortalized (28) and primary hepatic stellate cells, a known resident target cell type of CCL5 during liver fibrosis (13). Met-CCL5 is a

recombinant CCL5 analog, in which the initiating methionine residue is retained after recombinant production in prokaryotic cells, resulting in a potent antagonist of the murine CCL5 receptors CCR5 and CCR1 (20, 22). As depicted in Figure 5A, Met-CCL5 was able to significantly inhibit the migration of stellate cells toward Ccl5, an important biological aspect of stellate cells during fibrogenesis. Furthermore, Met-CCL5 significantly inhibited the Ccl5- and Ccl5/Tnf- α -induced secretion of Ccl2, a known profibrotic chemokine (10) (Figure 5B). As shown above, most Ccl5 is secreted by immune cells within the injured liver. We therefore investigated the direct effects of conditioned media derived from splenocyte cultures on the biologic behavior of hepatic stellate cells. When stellate cells were incubated with conditioned medium from WT-derived splenocytes, their migration, proliferation, and collagen secretion were strongly increased compared with those incubated with control medium. In contrast, all these features of stellate cells were strongly reduced by conditioned media obtained from splenocytes of *Ccl5*^{-/-} mice or pretreatment of stellate cells with Met-CCL5 (all $P < 0.01$; Figure 5, C-E). In contrast, the induction of apoptosis in stellate cells, as measured by Annexin-V positivity, was not changed by Met-CCL5 (Supplemental Figure 4A). Importantly,

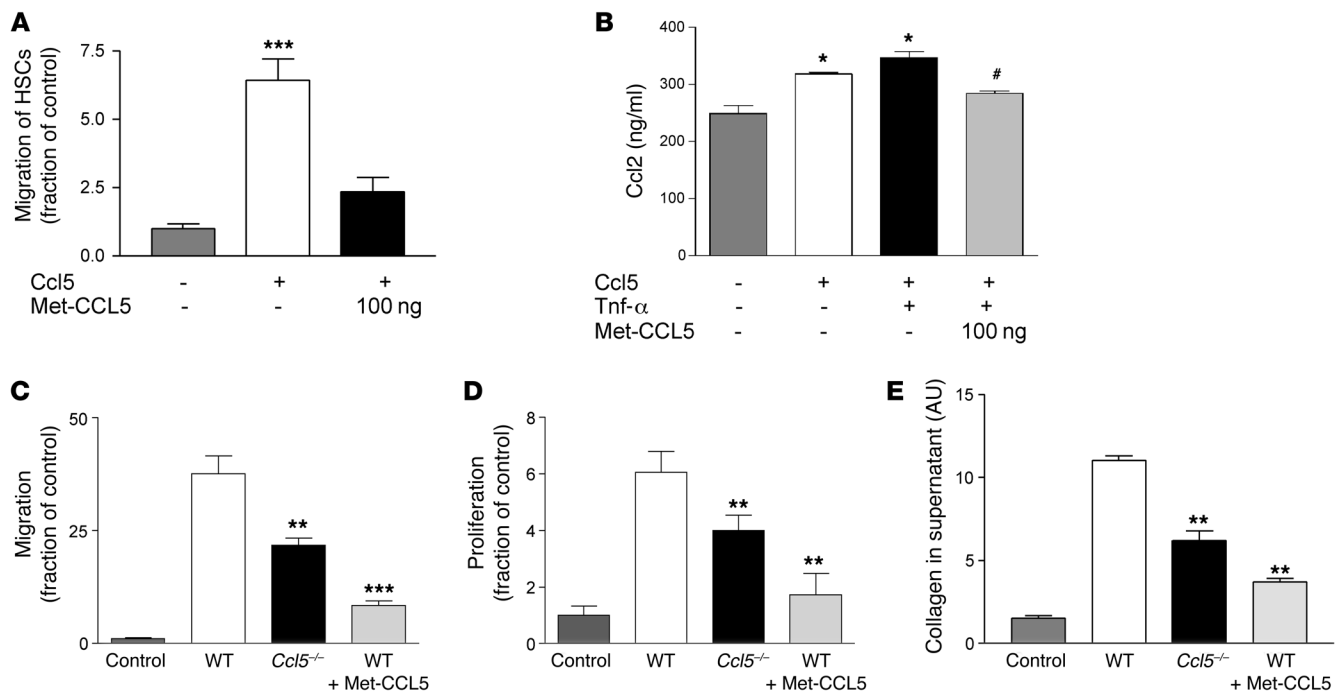


Figure 5

In vitro evidence for a role of Ccl5 in liver fibrosis. (A) Migration of stellate cells toward Ccl5 was assessed in Boyden chamber experiments. Stellate cells actively migrate toward Ccl5 ($***P < 0.001$, compared with medium), which is strongly inhibited by the pretreatment of the cells with Met-CCL5. (B) Ccl5 and Ccl5/Tnf- α stimulation of stellate cells leads to increased secretion of Ccl2 ($*P < 0.05$, versus unstimulated cells) after 24 hours, which can be significantly inhibited by Met-CCL5 ($\#P < 0.05$, versus Ccl5- and Ccl5/Tnf- α -stimulated cells). Supernatant from activated T cell-enriched splenocyte cultures of WT mice strongly stimulates the migration (C), proliferation (D), and collagen protein secretion (E) of stellate cells. These profibrotic phenotypes of stellate cells are severely blunted by supernatants from either splenocytes of Ccl5^{-/-} mice or pretreatment of stellate cells with Met-CCL5 ($**P < 0.01$, $***P < 0.001$). All in vitro experiments were performed at least twice in quadruplicates.

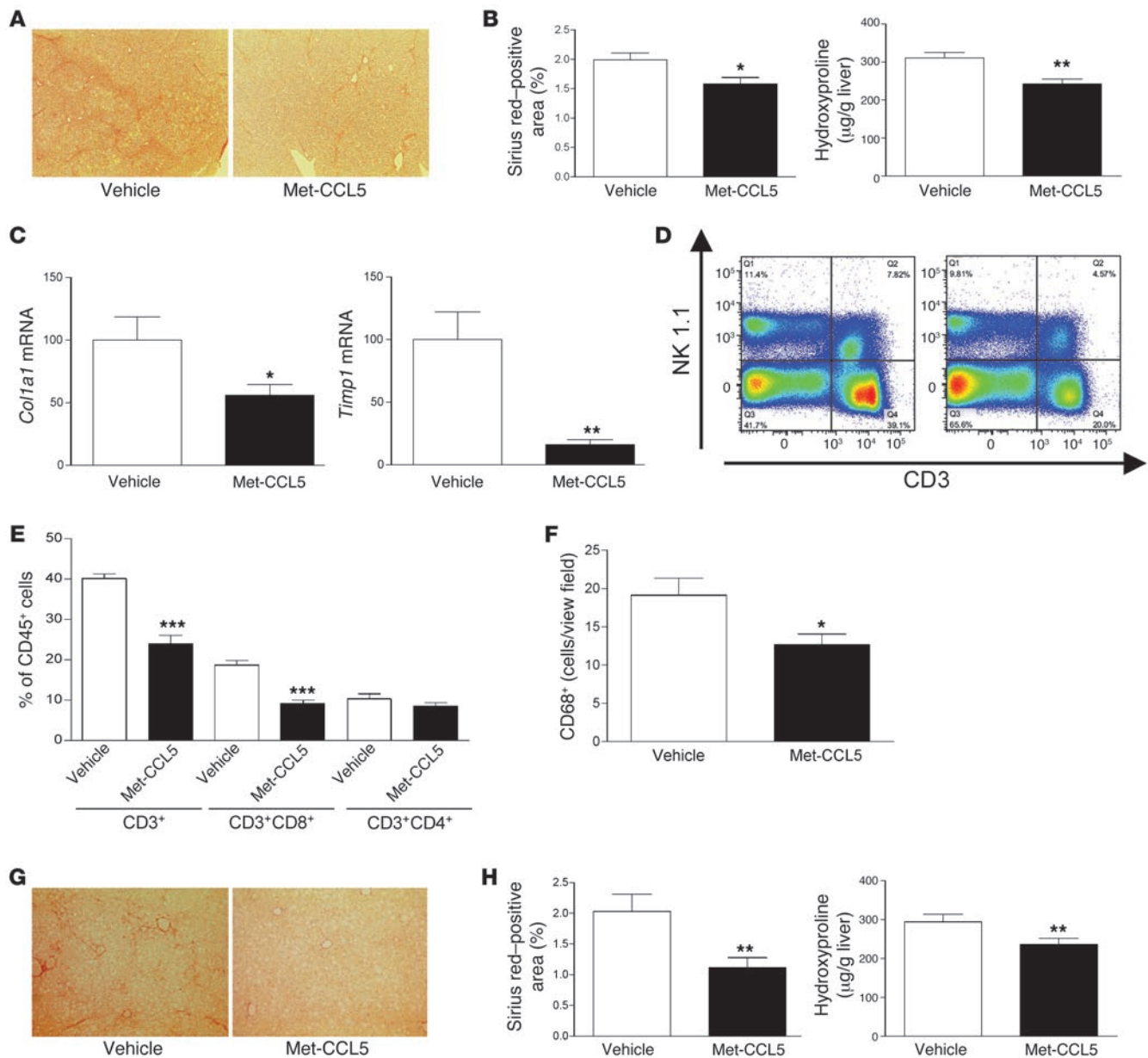
the results obtained in the immortalized stellate cells were reproduced in primary hepatic stellate cells, as evidenced by their collagen production and proliferation features in response to Ccl5 (Supplemental Figure 4, B and C). Taken together, these results suggested that the CCL5 antagonist, Met-CCL5, bears the potential to strongly inhibit the interaction between immune cells and stellate cells.

Pharmacological antagonism with Met-CCL5 reduces liver fibrosis in vivo. Based on these in vitro data, we evaluated whether pharmacological antagonism of CCL5 receptors by Met-CCL5 can alter the progression of liver fibrosis in vivo. We first administered Met-CCL5 (10 μ g) or vehicle daily to WT mice concomitantly with 12 CCL₄ injections over 6 weeks. Three days after the last CCL₄ injection, the animals were sacrificed and the fibrosis phenotype was evaluated. As depicted in Figure 6, A and B, mice treated with Met-CCL5 had strongly reduced liver scarring compared with that of vehicle-treated mice, as evidenced by quantification of the Sirius red-positive area and by biochemical measurement of liver hydroxyproline contents ($P < 0.05$ and $P < 0.01$, respectively). In accordance with the results obtained in the Ccl5^{-/-} mice and our in vitro data, the key profibrogenic genes *Coll1a1* and *Timp1* were significantly repressed by administration of Met-CCL5, compared with vehicle treatment (Figure 6C), as was the α -SMA protein expression (Supplemental Figure 5A). As CCL5 is a known chemoattractant for immune cells, we hypothesized that administration of Met-CCL5 should be accompanied by a changed inflammatory infiltrate in the injured livers. We therefore assessed the intrahepatic infiltration of immune cells by FACS analysis and immunohistochemistry.

While the numbers of NK and NKT cells were not strongly affected by the administration of Met-CCL5 (Figure 6D), T cells and, specifically, numbers of CD8⁺ T cells were greatly reduced in the Met-CCL5-treated mice compared with vehicle-treated mice ($P < 0.0001$, $P < 0.00001$, respectively; Figure 6E). Furthermore, the number of CD68⁺ macrophages was significantly reduced in Met-CCL5-treated animals (Figure 6F), while B220⁺ B cells and CD11c⁺ dendritic cells were not significantly changed compared with those of vehicle-treated mice (Supplemental Figure 5).

In order to confirm the antifibrotic effects of Met-CCL5, we subjected mice fed the MCD diet to daily Met-CCL5 (10 μ g/daily) or vehicle injections. As shown in Figure 6, G and H, Met-CCL5 was also able to significantly reduce liver fibrosis in this model, suggesting that antifibrotic effects by Met-CCL5 can be achieved in liver diseases of different etiologies. As in the other models, Met-CCL5 administration also led to reduced ALT levels and a repression of fibrosis-related genes (Supplemental Figure 6, A and B, respectively).

Met-CCL5 accelerates fibrosis regression in vivo. In the latter experiments, Met-CCL5 was administered concomitantly with the fibrotic stimulus and was thus shown to ameliorate the progression of liver scarring. In the next set of experiments, we tested the hypothesis that treatment of Met-CCL5 is also able to induce the regression of established liver fibrosis. For this purpose, C57BL/6 mice were challenged with CCL₄ for 8 weeks to establish severe fibrosis. Mice were then divided between a group that received daily Met-CCL5 injections during fibrosis regression and a group

**Figure 6**

In vivo inhibition of liver fibrosis by Met-CCL5. (A) Representative Sirius red stainings of CCl₄-treated C57BL/6 WT mice, with a concomitant administration of vehicle or Met-CCL5 ($n = 10/\text{group}$; original magnification, $\times 40$). (B) Reduced fibrosis in Met-CCL5-treated mice is validated by a significantly lower Sirius red-positive area ($*P < 0.05$) and decreased concentrations of hydroxyproline ($**P < 0.01$). (C) The reduced fibrotic response in Met-CCL5-treated mice is further evidenced by significantly reduced *Col1a1* and *Timp1* mRNA levels ($*P < 0.05$, $**P < 0.01$). (D) Representative FACS blot of NK1.1 and CD3-positive cell infiltration in vehicle- and Met-CCL5-treated animals, demonstrating a reduced T cell infiltration into the livers of Met-CCL5-treated mice, while numbers of NK and NKT cells are not significantly altered. (E) Statistical analysis of T cell infiltration (FACS) reveals a significantly reduced number of CD3- and, specifically, CD8-positive cells after treatment with Met-CCL5 ($***P < 0.001$). (F) In addition, numbers of CD68⁺-positive macrophages are also reduced in Met-CCL5-treated animals compared with those of vehicle-treated mice ($*P < 0.05$, $n = 10/\text{group}$). (G) The antifibrotic potential of Met-CCL5 is validated in the MCD fibrosis model by histology (original magnification, $\times 40$). (H) Reduced liver damage in Met-CCL5-treated mice is evidenced by a lower Sirius red-positive area in histology ($**P < 0.01$) and significantly reduced hydroxyproline levels ($**P < 0.01$) compared with those of vehicle-treated animals.

that received daily vehicle i.p. As depicted in Figure 7A, Met-CCL5 treatment indeed resulted in an accelerated resolution of liver scarring compared with those animals treated with vehicle. This difference was histologically evident after 7 days (Figure 7B), a finding that was confirmed by reduced hydroxyproline levels in

the Met-CCL5-treated mice at the same time point (Figure 7C; $P < 0.05$). The significant changes in collagen content in the livers of the Met-CCL5-treated mice after 7 days were preceded by repression of *Col1a1* and *Timp1* mRNA expression 3 days after the peak of fibrosis (Figure 7D; $P < 0.05$).

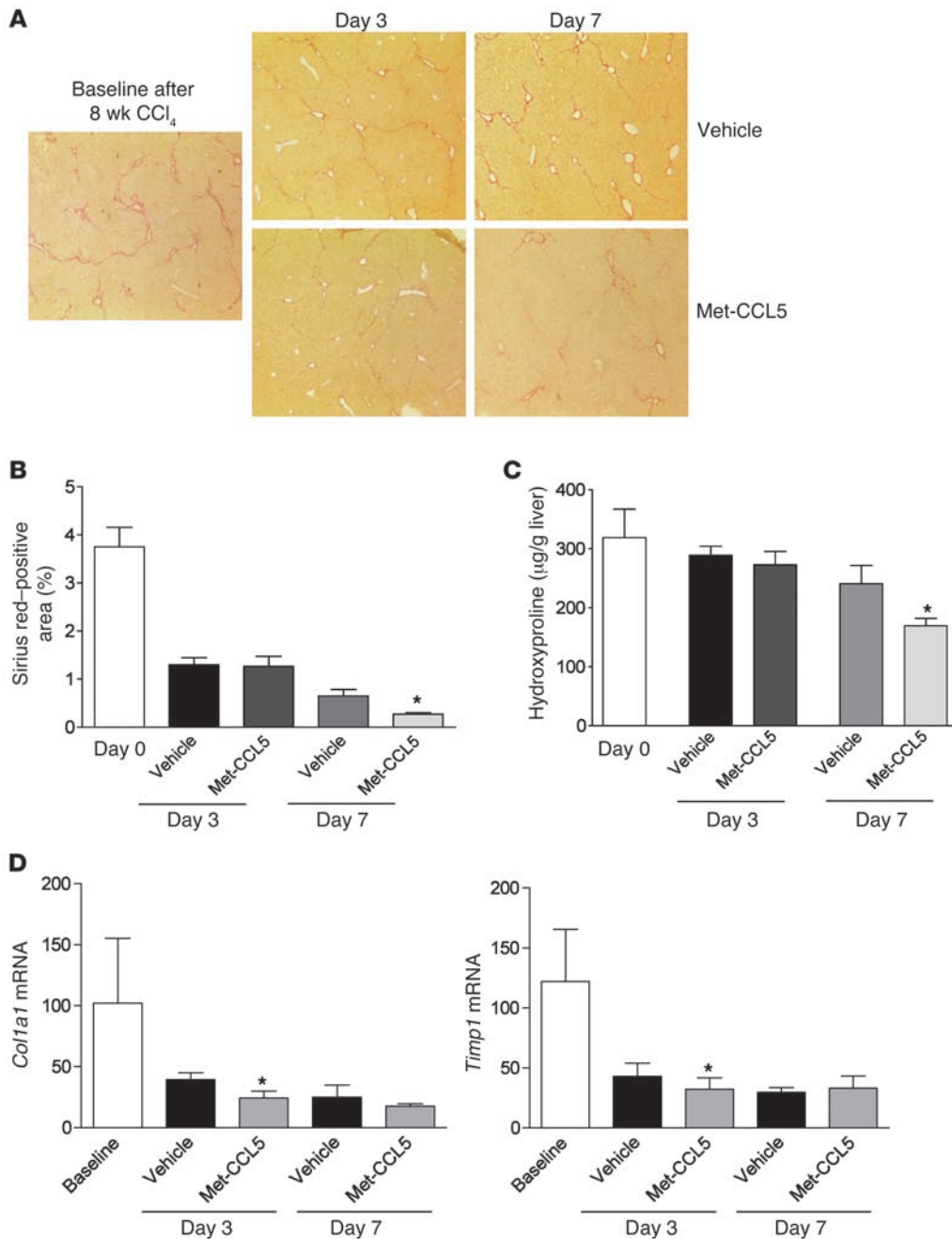


Figure 7 Met-CCL5 accelerates the regression of liver fibrosis in vivo. (A) C57BL/6 mice were challenged with CCl₄ for 8 weeks to establish advanced liver scarring. Three days after the last the last CCl₄ injection (at the peak of fibrosis), mice received either Met-CCL5 or vehicle (*n* = 8/group) and were assessed for fibrosis regression by histology for an overall duration of 7 days. At day 7, the mice that received Met-CCL5 displayed a significantly reduced residual fibrosis compared with the vehicle-treated group (original magnifications, ×40). (B) The difference between the groups is evidenced by a reduced Sirius red-positive area in the Met-CCL5-treated mice (**P* < 0.05) and (C) by significantly lower hydroxyproline contents at the same time point during fibrosis regression (**P* < 0.05). (D) Functionally, mRNA expression of *Col1a1* and *Timp1* is already significantly reduced at day 3, after start of Met-CCL5 or vehicle treatment (**P* < 0.05).

Discussion

Here we provide evidence that the CC chemokine CCL5 is a molecular mediator of liver fibrosis across different chronic liver diseases and that pharmacological antagonism of CCL5 receptors by Met-CCL5 is sufficient to reduce experimental liver scarring and enhance its regression in vivo.

Different lines of evidence were followed to demonstrate that CCL5 is intrinsically involved in liver fibrosis. The role of CCL5 was first evaluated in different human liver diseases using genetic and molecular analysis. Our haplotype analysis demonstrates a genetic association of functional CCL5 gene variants with the severity of liver fibrosis in HCV infection. Recent studies investigated only single-gene variants in the CCL5 promoter in patients with HCV infection (29, 30). These latter studies

reported an association of variants at positions -28 and -304 of the CCL5 gene, with the grade of inflammation in liver biopsy. However, single SNP studies are prone to over interpretation, as linkage disequilibrium at the genetic locus is not taken into account (31). We therefore chose haplotype analysis, with all tagging SNPs from the full data set of the HapMap project (32). Importantly, we replicated our genetic findings in an independent cohort. However, we could only detect a trend toward slightly higher CCL5 serum levels in carriers of the minor allele of the risk-associated tagging SNP. This suggests that genetically determined serum levels might only marginally contribute to the increased fibrosis in carriers of the risk allele and further studies on the functional importance of this SNP might be worthwhile.



In the second step of our analysis, we showed that the mRNA expression of *CCL5* is strongly associated with the presence of liver fibrosis. While this has already been suggested for HCV (12, 13, 33), our data is the first to our knowledge to show an association between a high levels of *CCL5* mRNA expression and the presence of fibrosis in fatty liver disease without HCV coinfection. Increased expression of *Ccl5* was also demonstrated at the mRNA and the protein level in animal models of toxic and metabolic liver fibrosis in the present study. The high level of mRNA expression in mice with liver damage is in line with that in a recent publication (13), while the protein levels have not yet been analyzed. However, in light of the expanding knowledge about microRNAs and other aspects of posttranslational gene regulation, it seemed mandatory to investigate chemokine protein levels. Importantly, we identified hematopoietic cells and, more specifically, T cells as a predominant source of Ccl5 protein within the injured liver by generating bone marrow chimeric mice and by immunohistochemistry. As T cells, together with macrophages, are known to secrete CCL5, these results support the hypothesis that infiltrating cells into the liver significantly contributes to the degree of tissue injury (6, 11).

However, the latter observations are associative in nature and can not differentiate causes and effects. We therefore analyzed *Ccl5*^{-/-} mice and their WT littermates for fibrosis progression in the well-established CCl₄ and MCD models of liver damage. These experiments were based on the a priori hypothesis that genetic deletion of *Ccl5* should lead to reduced liver scarring in vivo. As shown in Figure 3, *Ccl5*^{-/-} mice indeed had a greatly reduced propensity to develop severe fibrosis compared with their WT littermates. Notably, *Ccl5*^{-/-} mice also showed reduced ALT levels, suggesting that the inflammatory hepatocyte damage in the liver is also determined by Ccl5, apart from other mediators of the innate immune system, which need to be further defined (34).

Based on these results, we hypothesized that in our models infiltrating hematopoietic (immune) cells are the main source of Ccl5, while liver resident stellate cells should be a prime target for Ccl5. In order to clarify these hypotheses, we performed bone marrow transplantations from *Ccl5*^{-/-} mice into WT mice and vice versa. The results showed that deletion of *Ccl5* in liver resident cells only led to a moderate change in the fibrosis phenotype, while deletion of *Ccl5* from hematopoietic cells led to a strong reduction in liver scarring, as evidenced by histology, hydroxyproline, and fibrosis-relevant gene expression. These results are in accordance with data on atherosclerosis (18) and, indeed, supported our assumption that stellate cells are a target (15) rather than a source (8) of Ccl5 in CCl₄-induced fibrosis, which is in line with recent findings by Seki et al. (13). Nevertheless, in line with the known chemoattractant properties of Ccl5 (14), T cells and macrophages (which both express Ccl5 receptors) were also decreased in *Ccl5*-deficient mice or animals treated with Met-CCL5. This reduced T cell and macrophage infiltrate might lead to less hepatocellular collateral damage and, in turn, lower ALT levels, as consistently shown in all of our in vivo models.

We further investigated the direct effects of Ccl5 on primary and immortalized stellate cells (28). As shown in Figure 5, Ccl5 has a significant impact on the migration and proliferation of stellate cells, which were strongly inhibited by the CCL5 antagonist, Met-CCL5. Met-CCL5 was also able to significantly decrease the Ccl5-mediated release of Ccl2, a pivotal profibrotic chemokine produced by stellate cells. However, these experiments only inves-

tigate the effects of single molecules on the phenotype of stellate cells, while in vivo different molecules interact with each other. We therefore performed the crucial in vitro experiment on the effects of conditioned media from T cell-enriched splenocyte cultures on the proliferation, migration, and the collagen production of stellate cells. As shown in Figure 5, use of either splenocytes from *Ccl5*^{-/-} mice or pretreatment of stellate cells with Met-CCL5 indeed strongly inhibited all these fibrosis-associated phenotypes of stellate cells. These results reinforce the concept of a direct interaction between immune cells and stellate cells, which has recently been described as an important pathway in liver fibrosis (5). Based on our data, we show that Ccl5 secreted by immune cells is one of the main mediators of this interaction and that Ccl5 effects might be inhibited by Met-CCL5 in vivo.

This led us to the central experiment in which we administered Met-CCL5 to WT mice concomitantly with CCl₄ treatment or a MCD diet. As shown in Figure 6, the Met-CCL5-treated animals indeed developed significantly less liver injury compared with vehicle-treated animals. The effects of Met-CCL5 were evident at the histological, biochemical (hydroxyproline), and molecular (*Col1a1* and *Timp1* mRNA) level, suggesting a profound pharmacological effect of CCL5 receptor antagonism on liver scarring. Furthermore, we found a decreased infiltration of T cells (mainly CD8⁺ T cells) and macrophages in the livers of Met-CCL5-treated mice, which are believed to directly promote fibrosis (35, 36).

The latter experiments focused on the effects of Met-CCL5 on fibrosis progression, while the effects of chemokine antagonistic strategies during fibrosis regression are clinically more relevant. We therefore administered Met-CCL5 to mice, which were challenged with CCl₄ at the peak of fibrosis, and determined fibrosis regression in these animals compared with that of vehicle-treated animals. Under these circumstances, Met-CCL5 was indeed able to accelerate the regression of experimental fibrosis during follow-up (Figure 7), providing the rationale for further investigation of CCL5-antagonistic strategies in preclinical trials (37).

In summary, we here provide in vitro and in vivo evidence that the CC chemokine CCL5 is a critical mediator of experimental liver fibrosis. Crucially, we show that pharmacological antagonism of CCL5 receptors is sufficient to modulate the progression as well as the regression of liver scarring in vivo, thereby describing what we believe to be the first antifibrotic therapy, which antagonizes a single chemokine pathway in experimental liver diseases.

Methods

Human study population. Overall, 211 patients of European descent with chronic HCV infection were included in the genetic analysis (23). Chronic HCV infection was diagnosed based on a positive anti-HCV test (Abbott) and a positive HCV-RNA test (Roche). In all subjects, other liver diseases were excluded by appropriate serological test. None of the patients had an average alcohol intake of more than 20 g per day. In all patients, liver biopsy was performed prior to antiviral therapy, and fibrosis and inflammation were scored by a single pathologist, according to the Desmet and Scheuer scoring system as described previously (38). An independent cohort of patients of European descent from the Department of Gastroenterology at the Charité University Hospital served as a validation sample for the genetic analysis.

Furthermore, total hepatic mRNA was isolated from 54 patients with chronic HCV infection, 20 patients with fatty liver, and 22 subjects with NASH who underwent liver biopsy for staging of their disease as described previously (11). We also determined the CCL5 serum concentration in



serum samples from 72 patients with chronic hepatitis C in relation to the *CCL5* genotype using *CCL5* ELISA (R&D Systems). Patients gave informed consent prior to inclusion in the studies, and the protocols were approved by the ethics committee at the Universities of Aachen and Berlin.

Human genetic analysis. We identified 2 SNPs from the complete data set of the International HapMap project, which covers the genetic information of the *CCL5* gene on chromosome 17 with Haploview 4.0 (<http://hapmap.ncbi.nlm.nih.gov/>). These SNPs (rs2291299 and rs11652536) were genotyped using 5'-endonuclease (TaqMan) assays with Assays-on-Demand from Applied Biosystems. The genotypic data was then uploaded into PHASE 2.0 (24), and haplotypes were inferred. The distribution of these haplotypes between patients with mild fibrosis (F0/F1) and advanced fibrosis (F2–F4) was compared by permutation testing, which formally corrects for multiple testing in the screening cohort from the University of Aachen (24). After having shown a significant difference in haplotype distribution, the frequency of the specific haplotypes (*CCL5_H1* to *CCL5_H4*) was compared using Fisher's exact test among the cohorts with different severity of fibrosis, and the OR of having severe fibrosis in carriers of the at-risk alleles was calculated. Haplotypes were named, according to their frequency, from *CCL5_H1* to *CCL5_H4*. In the validation cohort, the *CCL5_H3* haplotype tagging SNP rs11652536 was genotyped, and data was analyzed with genetic software provided by Institute of Human Genetics, Technical University Munich, Munich, Germany (<http://ihg.gsf.de>).

Expression analysis of *CCL5* mRNA in human liver biopsies. Total liver RNA was isolated and reversely transcribed using SuperScript (Invitrogen), as described previously (11). Quantitative RT-PCR was carried out for *CCL5* with an Assay-on-Demand (Applied Biosystems).

Murine *in vivo* experiments. Mice with a targeted deletion of the *Ccl5* gene (*Ccl5*^{-/-} mice) were obtained from The Jackson Laboratory and backcrossed onto the C57BL/6 background for more than 10 generations. Animal care and experiments were performed after written approval of the experiments by the Animal Experiments Review Board of the Bezirksregierung Cologne, Germany. Littermates with WT *Ccl5* on the C57BL/6 background served as controls. The *Ccl5*^{-/-} mice used in our study had no morphologically or functionally overt abnormal phenotype, but a reduced T cell proliferation has been described in these animals (39).

Mice were subjected to 2 different fibrosis models. In the first model, *Ccl5*^{-/-} and WT mice ($n = 12$ mice per group) received intraperitoneal injections of CCL₄ for 6 weeks (0.6 mg/kg, twice weekly). Mice were sacrificed 3 days after the last injection. In the second model, *Ccl5*^{-/-} and WT mice ($n = 12$ mice per group) were fed a MCD diet (MP Biomedicals Europe) for 8 weeks, which is an established model of NASH (40).

In a separate experiment, C57BL/6 WT mice received CCL₄ injections for 6 weeks and were treated in parallel with 10 µg Met-CCL5 i.p. or saline i.p. daily. Met-CCL5 is a selective antagonist of the CCL5 receptors CCR1 and CCR5. Its synthesis has been described before by our groups (16, 41). The *in vivo* dose of Met-CCL5 was chosen based on our experience in animal models of atherosclerosis (18). Mice were sacrificed 3 days after the last CCL₄ injection for further analysis. The same protocol of Met-CCL5 administration was used during an 8-week feeding experiment with the MCD diet to induce metabolic liver fibrosis ($n = 10$ mice/group).

In another set of experiments, C57BL/6 WT mice received CCL₄ injections for 8 weeks to establish pronounced fibrosis. CCL₄ was then stopped, and the peak of fibrosis was calculated to occur 3 days after the last CCL₄ injection (day 0 of fibrosis regression). Liver fibrosis regression was then monitored 3 and 7 days after the peak of fibrosis in mice, which received either Met-CCL5 (10 µg/d) or vehicle ($n = 8$ mice/group/time point) during fibrosis regression.

In all animals, liver fibrosis was assessed histologically by quantification of the Sirius red-positive area on 10 low-power (magnification, ×40) fields per slide, with use of the NIH ImageJ software (<http://rsbweb.nih.gov/>). Liver

fibrosis was also assessed biochemically by photometric measurement of the collagen-specific amino acid hydroxyproline, as described previously (42).

***Ccl5* ELISA and α -SMA Western blot.** Snap-frozen liver samples were incubated for 30 minutes in 1 ml RIPA buffer (20 mM Tris-HCl, 150 mM NaCl, 2% Nonidet P40, 0.1% SDS, 0.5% Na-deoxycholate) with proteinase inhibitor (Mini Complete Protease Inhibitor Cocktail Tablets, Roche Applied Science) for isolation of total protein. Analysis of intrahepatic Ccl5 was performed using a murine ELISA (R&D Systems) in duplicate, following the manufacturer's instructions. Intrahepatic Ccl5 concentrations are expressed in pg per mg of total liver protein.

Western blotting of α -SMA was performed from total liver protein, using a monoclonal mouse anti-mouse α -SMA antibody (Millipore). The primary antibody was visualized using horseradish peroxidase-conjugated anti-mouse IgG (DAKO) and the SuperSignal Chemiluminescent Substrate (Thermo Fisher Scientific). GAPDH was used as loading control.

Hepatic triglyceride levels. The hepatic triglyceride content was determined in homogenized liver tissue. The standard curve was prepared according to the assay protocol of Triglyceride liquicolor mono assay (Human Diagnostics). Two µg of each liver sample were put into a 96-well ELISA plate. After adding 200 µl of the kit reagent, the samples were incubated at room temperature for 45 minutes. Within a 60-minute incubation period, the samples were measured at 492 nm OD.

Immunofluorescence staining of murine liver tissue. Immunofluorescence staining of Ccl5 was performed with a polyclonal goat anti-mouse Ccl5 antibody (sc-1410, Santa Cruz Biotechnology Inc.) on acetone-fixed 5-µm cryosections of liver tissue. Costaining for CD3 was performed with a rat anti-mouse CD3 antibody (ABD Serotec). Staining for α -SMA was performed with a monoclonal mouse anti-mouse α -SMA antibody (Millipore).

To analyze the intrahepatic content of macrophages, B cells, and dendritic cells, sections were stained using a monoclonal rat anti-mouse CD68 antibody (ABD Serotec), a monoclonal rat anti-mouse B220 antibody (Cederlane Laboratories), or a monoclonal Armenian hamster anti-CD11c antibody (eBioscience). All staining were controlled by appropriate isotype controls.

Bone marrow transplantation. We transferred the bone marrow of *Ccl5*^{-/-} or WT mice ($n = 7$ –8/group) into 6- to 8-week-old recipients (all on the C57BL/6J background) after ablative γ -irradiation, as described previously (18). After 4 weeks of reconstitution, mice were subjected to 6 weeks of treatment with CCL₄, as described above.

Expression analysis of *CCL5* and murine fibrosis-related genes. Total RNA was isolated from livers of mice and reverse transcribed using SuperScript (Invitrogen). Quantitative RT-PCR was carried out for *Ccl5*, *Colla1*, *Timp1*, *Tgfb1*, *Mmp9*, and *Il6* with Assays-on-Demand (Applied Biosystems).

Hepatic immune cell isolation and flow cytometry analysis. Single-cell suspensions were isolated from freshly harvested livers using mechanical and enzymatic digestion. Viable white blood cells were purified from the suspension by centrifugation for 20 minutes at 800 g, with a density gradient separation medium (Lympholyte-H, Cederlane Laboratories). PBMCs were collected from the gradient/supernatant interface and then washed in Hank's balanced salt solution supplemented with 1% bovine serum albumin and 2 mM EDTA. For flow cytometry analysis, cells were stained with fluorochrome-conjugated antibodies for CD45, CD3, CD4, CD8, and NK1.1 (eBioscience), and the relative numbers were quantified using the FACSCanto II (Becton Dickinson). Data were analyzed using FlowJo software (Tree Star).

Cell migration assay. Cell migration assays were performed using a modified Boyden chamber. Briefly, stellate cells (4×10^4 cells/well) were placed in the upper chamber in DMEM, without FCS, and with or without preincubation with 100 ng Met-CCL5 for 30 minutes and exposed to recombinant murine Ccl5 (20 ng) in the lower chamber. The *in vitro* dose of Met-CCL5 was adjusted to the minimal effective dose over a concentration gradient



from 1 to 1,000 ng/ml. In a separate experiment, stellate cells were exposed to either conditioned medium from splenocytes isolated from WT mice, with or without Met-CCL5 (100 ng/ml), or conditioned medium from *Ccl5*^{-/-} splenocytes (see below) in the lower chamber. After 4 hours of incubation at 37°C, cells that migrated to the lower chamber were counted in 6 randomly chosen (magnification, ×100) fields. All experiments were replicated at least twice in quadruplicates.

Stimulation of the murine stellate cell line GRX with *Ccl5* and Met-CCL5. Culture of the murine hepatic stellate cell line GRX has been described previously (28). For chemokine stimulation, cells were starved for 24 hours in DMEM (PAA Laboratories) containing 1% fetal calf serum and stimulated with 20 ng/ml recombinant murine Ccl5 alone or in combination with 0.25 ng/ml TNF- α (both R&D Systems), with or without 100 ng/ml Met-CCL5, for 24 hours. Ccl2 concentrations were determined in supernatants using a murine ELISA (R&D Systems) in duplicate following the manufacturer's instructions. Ccl2 concentrations are given in pg per ml supernatant.

Cell proliferation assay. Proliferation of primary or immortalized hepatic stellate cells was assessed by a colorimetric immunoassay based on the measurement of BrdU incorporation during DNA synthesis (Cell Proliferation ELISA, Roche Applied Science) following the manufacturer's instructions. Briefly, cells were starved for 16 hours in DMEM medium (PAA Laboratories) without fetal calf serum and stimulated for 24 hours with either conditioned medium from WT splenocytes, with or without Met-CCL5 (100 ng/ml), or conditioned medium from *Ccl5*^{-/-} splenocytes (see below). After preincubation, cells were labeled with BrdU for 2 hours. BrdU incorporation was assessed after removal of labeling media, fixation of cells, and DNA denaturation by adding an anti-BrdU peroxidase antibody and measuring the subsequent substrate reaction.

Splenocyte isolation and stimulation of GRX cells with conditioned media. Splenocytes from *Ccl5*^{-/-} and WT mice were isolated using standard protocols. Cells were cultured for 24 hours and transferred to another tissue culture flask, diminishing the percentage of adherent cells. After counting of cells, the cell concentration was adjusted to 2×10^6 cells per ml. For conditioned media, splenocyte suspension of *Ccl5*^{-/-} or WT mice was incubated for 48 hours with 10 μ g/ml Concanavalin A (Sigma-Aldrich) and filtered through a PES membrane (Nalgene; 0.1- μ m mesh diameter) to remove cells and debris. Cultured

GRX cells were incubated for 24 hours with either conditioned medium from splenocytes of WT mice, with or without pretreatment with Met-CCL5 (100 ng/ml) for 30 minutes, or conditioned medium from *Ccl5*^{-/-} splenocytes. Supernatant was obtained, and the collagen concentration was assessed by Western blot analysis with a polyclonal rabbit anti-murine collagen type I antibody (Monosan). The primary antibody was visualized using horseradish peroxidase-conjugated anti-rabbit IgG (DAKO) and the SuperSignal Chemiluminescent Substrate (Thermo Fisher Scientific). Semiquantitative analysis of the bands was performed with Quantity One software (Bio-Rad).

Isolation and culture of primary murine hepatic stellate cells. Primary hepatic stellate cells were isolated from C57BL/6 mice and *Ccl5*^{-/-} mice, as previously described by our group (43). After isolation, cells were cultured in DMEM (PAA Laboratories) supplemented with 10% fetal calf serum (Biocrom KG), 4 mM L-glutamine (PAA Laboratories), 100 IU/ml penicillin, and 100 μ g/ml streptomycin (PAA Laboratories). The medium was changed 1 day after initial plating and thereafter every third day, while cultures were maintained at 37°C, 5% CO₂, in a humidified atmosphere.

Statistics. Data are given as mean \pm SEM. Continuous variables were compared by 2-sided *t* tests, with Welch's correction in case of unequal variances. Variables in contingency tables were compared by Fisher's exact test, with which we also calculated ORs for the genetic analysis. *P* values of less than 0.05 were considered significant in all analyses. Statistical tests were performed using GraphPad Prism 4.0.

Acknowledgments

The study was supported by grants from the Deutsche Forschungsgemeinschaft (SFB/TRR 57) and the Medical Faculty of the University of Aachen (START and IZKF grants to H.E. Wasmuth).

Received for publication November 11, 2009, and accepted in revised form September 1, 2010.

Address correspondence to: Hermann E. Wasmuth, Medical Department III, University Hospital Aachen, RWTH Aachen, Pauwelsstrasse 30, D-52057 Aachen, Germany. Phone: 49.241.8080861; Fax: 49.241.8082455; E-mail: hwasmuth@ukaachen.de.

- Friedman SL. Mechanisms of hepatic fibrogenesis. *Gastroenterology*. 2008;134(6):1655–1669.
- Bataller R, Brenner DA. Liver fibrosis. *J Clin Invest*. 2005;115(2):209–218.
- Iredale JP. Models of liver fibrosis: exploring the dynamic nature of inflammation and repair in a solid organ. *J Clin Invest*. 2007;117(3):539–548.
- Fallowfield JA, Kendall TJ, Iredale JP. Reversal of fibrosis: no longer a pipe dream? *Clin Liver Dis*. 2006;10(3):481–497, viii.
- Holt AP, Salmon M, Buckley CD, Adams DH. Immune interactions in hepatic fibrosis. *Clin Liver Dis*. 2008;12(4):861–882, x.
- Marra F, Aleffi S, Galastri S, Provenzano A. Mononuclear cells in liver fibrosis. *Semin Immunopathol*. 2009;31(3):345–358.
- Karlmarm KR, Wasmuth HE, Trautwein C, Tacke F. Chemokine-directed immune cell infiltration in acute and chronic liver disease. *Expert Rev Gastroenterol Hepatol*. 2008;2(2):233–242.
- Holt AP, Houghton EL, Lalor PF, Filer A, Buckley CD, Adams DH. Liver myofibroblasts regulate infiltration and positioning of lymphocytes in human liver. *Gastroenterology*. 2009;136(2):705–714.
- Marra F, Valente AJ, Pinzani M, Abboud HE. Cultured human liver fat-storing cells produce monocyte chemoattractant protein-1. Regulation by proinflammatory cytokines. *J Clin Invest*. 1993; 92(4):1674–1680.
- Marra F, et al. Increased expression of monocyte chemoattractant protein-1 during active hepatic fibrogenesis: correlation with monocyte infiltration. *Am J Pathol*. 1998;152(2):423–430.
- Wasmuth HE, et al. Antifibrotic effects of CXCL9 and its receptor CXCR3 in livers of mice and humans. *Gastroenterology*. 2009;137(1):309–319.
- Nischalke HD, Nattermann J, Fischer HP, Sauerbruch T, Spengler U, Dumoulin FL. Semiquantitative analysis of intrahepatic CC-chemokine mRNAs in chronic hepatitis C. *Mediators Inflamm*. 2004;13(5-6):357–359.
- Seki E, et al. CCR1 and CCR5 promote hepatic fibrosis in mice. *J Clin Invest*. 2009;119(7):1858–1870.
- Appay V, Rowland-Jones SL. RANTES: a versatile and controversial chemokine. *Trends Immunol*. 2001;22(2):83–87.
- Schwabe RF, Bataller R, Brenner DA. Human hepatic stellate cells express CCR5 and RANTES to induce proliferation and migration. *Am J Physiol Gastrointest Liver Physiol*. 2003;285(5):G949–G958.
- Ajuebor MN, Wondimu Z, Hogaboam CM, Le T, Proudfoot AE, Swain MG. CCR5 deficiency drives enhanced natural killer cell trafficking to and activation within the liver in murine T cell-mediated hepatitis. *Am J Pathol*. 2007;170(6):1975–1988.
- Ajuebor MN, Hogaboam CM, Le T, Proudfoot AE, Swain MG. CCL3/MIP-1 α is pro-inflammatory in murine T cell-mediated hepatitis by recruiting CCR1-expressing CD4(+) T cells to the liver. *Eur J Immunol*. 2004;34(10):2907–2918.
- Koenen RR, et al. Disrupting functional interactions between platelet chemokines inhibits atherosclerosis in hyperlipidemic mice. *Nat Med*. 2009;15(1):97–103.
- Wu H, et al. T-cell accumulation and regulated on activation, normal T cell expressed and secreted upregulation in adipose tissue in obesity. *Circulation*. 2007;115(8):1029–1038.
- Proudfoot AE, et al. Extension of recombinant human RANTES by the retention of the initiating methionine produces a potent antagonist. *J Biol Chem*. 1996;271(5):2599–2603.
- Grone HJ, et al. Met-RANTES reduces vascular and tubular damage during acute renal transplant rejection: blocking monocyte arrest and recruitment. *FASEB J*. 1999;13(11):1371–1383.
- Chvatchko Y, et al. Inhibition of airway inflammation by amino-terminally modified RANTES/CC chemokine ligand 5 analogues is not mediated through CCR3. *J Immunol*. 2003;171(10):5498–5506.
- Berres ML, et al. A functional variation in CHI3L1 is associated with severity of liver fibrosis and YKL-40 serum levels in chronic hepatitis C infection. *J Hepatol*. 2009;50(2):370–376.
- Stephens M, Donnelly P. A comparison of Bayesian methods for haplotype reconstruction from population genotype data. *Am J Hum Genet*. 2003; 73(5):1162–1169.
- An P, et al. Modulating influence on HIV/AIDS by interacting RANTES gene variants. *Proc Natl Acad*



- Sci U S A*. 2002;99(15):10002–10007.
26. Streetz KL, et al. Interleukin 6/gp130-dependent pathways are protective during chronic liver diseases. *Hepatology*. 2003;38(1):218–229.
27. Friedman SL. Hepatic stellate cells: protean, multifunctional, and enigmatic cells of the liver. *Physiol Rev*. 2008;88(1):125–172.
28. Vicente CP, Fortuna VA, Margis R, Trugo L, Borojevic R. Retinol uptake and metabolism, and cellular retinol binding protein expression in an in vitro model of hepatic stellate cells. *Mol Cell Biochem*. 1998;187(1–2):11–21.
29. Promrat K, et al. Associations of chemokine system polymorphisms with clinical outcomes and treatment responses of chronic hepatitis C. *Gastroenterology*. 2003;124(2):352–360.
30. Hellier S, et al. Association of genetic variants of the chemokine receptor CCR5 and its ligands, RANTES and MCP-2, with outcome of HCV infection. *Hepatology*. 2003;38(6):1468–1476.
31. Wasmuth HE, Matern S, Lammert F. From genotypes to haplotypes in hepatobiliary diseases: one plus one equals (sometimes) more than two. *Hepatology*. 2004;39(3):604–607.
32. Frazer KA, et al. A second generation human haplotype map of over 3.1 million SNPs. *Nature*. 2007;449(7164):851–861.
33. Haybaeck J, et al. A lymphotoxin-driven pathway to hepatocellular carcinoma. *Cancer Cell*. 2009;16(4):295–308.
34. Seki E, et al. TLR4 enhances TGF-beta signaling and hepatic fibrosis. *Nat Med*. 2007;13(11):1324–1332.
35. Duffield JS, et al. Selective depletion of macrophages reveals distinct, opposing roles during liver injury and repair. *J Clin Invest*. 2005;115(1):56–65.
36. Safadi R, et al. Immune stimulation of hepatic fibrogenesis by CD8 cells and attenuation by transgenic interleukin-10 from hepatocytes. *Gastroenterology*. 2004;127(3):870–882.
37. Pinzani M, Vizzutti F. Fibrosis and cirrhosis reversibility: clinical features and implications. *Clin Liver Dis*. 2008;12(4):901–913, x.
38. Wasmuth HE, et al. Haplotype-tagging RANTES gene variants influence response to antiviral therapy in chronic hepatitis C. *Hepatology*. 2004;40(2):327–334.
39. Makino Y, et al. Impaired T cell function in RANTES-deficient mice. *Clin Immunol*. 2002;102(3):302–309.
40. Rangnekar AS, Lammert F, Igoznikov A, Green RM. Quantitative trait loci analysis of mice administered the methionine-choline deficient dietary model of experimental steatohepatitis. *Liver Int*. 2006;26(8):1000–1005.
41. Schober A, et al. Deposition of platelet RANTES triggering monocyte recruitment requires P-selectin and is involved in neointima formation after arterial injury. *Circulation*. 2002;106(12):1523–1529.
42. Hillebrandt S, et al. Complement factor 5 is a quantitative trait gene that modifies liver fibrogenesis in mice and humans. *Nat Genet*. 2005;37(8):835–843.
43. Weiskirchen R, Gressner AM. Isolation and culture of hepatic stellate cells. *Methods Mol Med*. 2005;117:99–113.